Robust dx2−y2 pairing symmetry in hole-doped cuprate superconductors

C. C. Tsuei, John R. Kirtley, German Hammerl, Jochen Mannhart, H. Raffy, Z. Z. Li

Angaben zur Veröffentlichung / Publication details:

Tsuei, C. C., John R. Kirtley, German Hammerl, Jochen Mannhart, H. Raffy, and Z. Z. Li. 2004. "Robust dx2−y2 pairing symmetry in hole-doped cuprate superconductors." Physical Review Letters 93 (18): 187004. https://doi.org/10.1103/physrevlett.93.187004.

Robust $d_{x^2-y^2}$ Pairing Symmetry in Hole-Doped Cuprate Superconductors

C. C. Tsuei,[1] J. R. Kirtley,[1] G. Hammerl,[2] J. Mannhart,[2] H. Raffy,[3] and Z. Z. Li[3]

[1]*IBM Watson Research Center, Yorktown Heights, New York, USA*

[2]*Experimental Physics VI, Center for Electronic Correlations and Magnetism, Institute of Physics, University of Augsburg, D-86135 Augsburg, Germany*

[3]*Laboratoire de Physique des Solides, Bâtiment 510, UMR 8502, Université Paris-Sud, 91405 Orsay, France*

(Received 25 February 2004; published 27 October 2004)

Although initially quite controversial, it is now widely accepted that the Cooper pairs in optimally doped cuprate superconductors have predominantly $d_{x^2-y^2}$ wave function symmetry, and the controversy has now shifted to whether the pairing symmetry changes away from optimal doping. Here we present phase-sensitive tricrystal experiments on three cuprate systems: $Y_{0.7}Ca_{0.3}Ba_2Cu_3O_{7-\delta}$ (Ca-doped Y-123), $La_{2-x}Sr_xCuO_4$ (La-214), and $Bi_2Sr_2CaCu_2O_{8+\delta}$ (Bi-2212), with doping levels covering the underdoped, optimal, and overdoped regions. Our work implies that predominantly $d_{x^2-y^2}$ pairing symmetry is robust over a large variation in doping.

DOI: 10.1103/PhysRevLett.93.187004 PACS numbers: 74.72.–h, 73.40.Gk, 74.20.–z, 74.50.+r

Doping with electrons or holes converts the cuprate perovskites from antiferromagnetic insulators to high-temperature superconductors with a superconducting transition temperature T_c [1] that can be described for many hole-doped cuprates by the empirical formula [2]

$$T_c(p) = T_{c,\max}[1 - 82.6(p - p_c)^2], \quad (1)$$

where p is the holes per CuO_2 layer and $p_c \approx 0.16$. Optimal doping is a watershed in many properties of the cuprate superconductors [1]. Nanometer-scale charge inhomogeneity, pseudogap, and other anomalous normal-state properties are observed mostly in the underdoped region, while overdoped cuprates appear to be Fermi liquids [1]. Moreover, the Hall number [3], superfluid pair density [4], and many other properties also depend remarkably on doping. In the language of quantum criticality [5], there are a number of competing states near the quantum critical point ($\approx p_c$). Variation in doping may induce a spin density or charge density wave phase, or a superconducting phase with different pairing symmetry, such as the time-reversal symmetry breaking (TRSB) pair states $d_{x^2-y^2} + is$ or $d_{x^2-y^2} + id_{xy}$ [6].

Although $d_{x^2-y^2}$ pairing symmetry is well established for several optimally doped cuprate superconductors [7], and some penetration depth measurements have indicated doping independent pairing symmetry [8], there are several studies suggesting a doping-induced change in pairing symmetry in some cuprates. For example, tunneling spectroscopy suggests a significant gapped (s-wave) component in the pairing wave function in overdoped $Y_{1-x}Ca_xBa_2Cu_3O_{7-\delta}$ [9], and a change in symmetry from $d_{x^2-y^2}$ to $d_{x^2-y^2} + id_{xy}$ or $d_{x^2-y^2} + is$ in overdoped $YBa_2Cu_3O_7$ [10]. One penetration depth measurement in electron-doped $Pr_{2-x}Ce_xCuO_4$ indicated a d to s transition in the optimal to overdoped range [11], although a second study indicated d-wave pairing at all doping levels studied in this system [12]. In addition, the low-temperature limit of the thermal conductivity expected for a d-wave superconductor [13] was observed in $La_{2-x}Sr_xCuO_4$ for all doping levels [14].

Phase-sensitive tests of pairing symmetry using the tricrystal geometry have been described elsewhere [7]. Briefly, thin films of cuprate superconductors are epitaxially grown on a $SrTiO_3$ substrate composed of three grains. The substrate and subsequent cuprate thin film geometry is chosen [Fig. 1(a)] such that, for a $d_{x^2-y^2}$ superconductor, in the absence of supercurrents there are an odd number of sign changes in the component of the pairing wave function normal to the grain boundaries upon circling the tricrystal point. The sign changes at the grain boundary interfaces cost Josephson coupling energy. This energy is reduced by the generation of time-reversal symmetric circulating supercurrents, resulting in a doubly degenerate Josephson vortex with a vortex number $N_\phi = +1/2$ or $-1/2$. For real superconducting order parameters and the conventional $I_s = I_1 \sin(\Delta\theta)$ Josephson current-phase relationship the tricrystal vortex should have exactly half of the conventional flux quantum $\phi_0 = h/2e = 2.07 \times 10^{-15}$ Wb of magnetic flux. In our geometry [Fig. 1(a)], a spontaneous $N_\phi = 1/2$ vortex will occur at the tricrystal point only if the $d_{x^2-y^2}$ component is at least as large as a possible s component. Further, an imaginary component to the order parameter would make the flux in the $N_\phi = 1/2$ vortex different from $\phi_0/2$; if this imaginary component had fixed sign the flux in the $N_\phi = \pm 1/2$ vortices would be different from each other. In both cases these differences divided by ϕ_0 would be approximated by the ratio of the imaginary component to the total pairing amplitude. The $N_\phi = \pm 1/2$ vortices at the tricrystal point could have the same absolute values of flux, if the sign of the imaginary component for the entire superconductor switched upon inversion, or if there were domains with imaginary order parameter components, but such domains would have to alternate signs on a

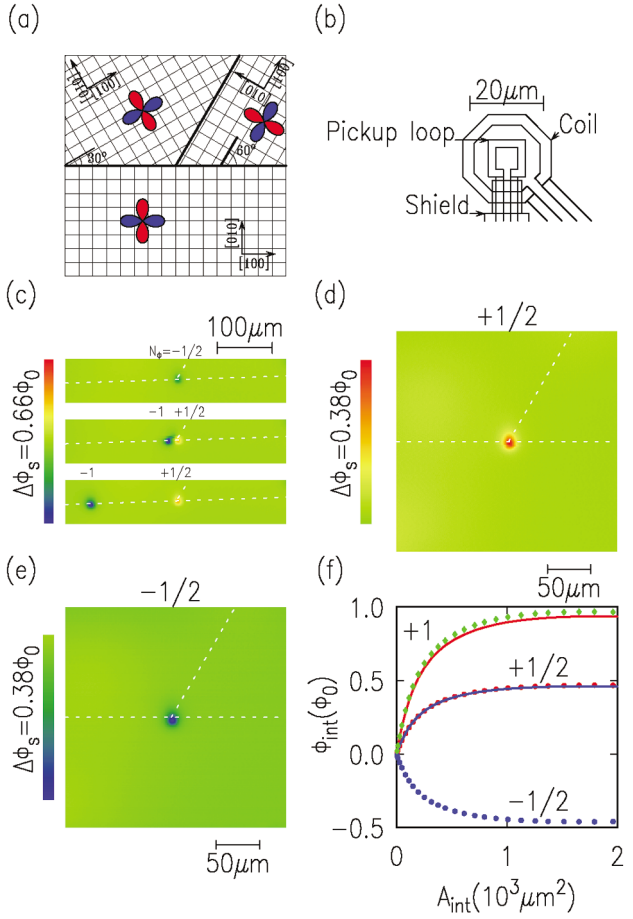

FIG. 1 (color). (a) Tricrystal geometry. The polar plots represent the pairing wave functions, with the red lobe phases shifted by π relative to the blue. (b) Schematic of the pickup loop area of the SQUID susceptometer sensor used. (c),(d),(e) are SQUID microscope images of the tricrystal point of a $Y_{0.7}Ca_{0.3}Ba_2Cu_3O_{7-\delta}$ film on a $SrTiO_3$ tricrystal with the geometry of (a). All SSM images in this Letter were taken at 4.2 K. The dashed lines indicate grain boundaries. (c) illustrates the inversion of a $N_\phi = -1/2$ vortex at the tricrystal point (top image). [(c), middle image] a 5 mA pulse of current is passed through the susceptometer field coil to invert a $-1/2$ vortex [(c), top image] to a $+1/2$ vortex, creating also a $N_\phi = -1$ Josephson vortex in the horizontal grain boundary. [(c), bottom image] the -1 Josephson vortex is dragged from the tricrystal point by moving the sensor parallel to the grain boundary while applying a current of 4 mA. $\Delta\phi_s$ is the net variation in flux through the SQUID pickup loop. (f) Shows the integration of the total flux (in units of ϕ_0) of the $N_\phi = +1/2$ state [(d), red dots], the $-1/2$ state [(e), blue dots], and a nearby $N_\phi = +1$ integer vortex (green dots) over a circular area $A_{\rm int}$ centered at the tricrystal point. The blue line in (f) is the $N_\phi = -1/2$ data multiplied by -1, demonstrating double degeneracy. The red line in (f) is the $N_\phi = +1/2$ data multiplied by 2.

length scale smaller than the experimental spatial resolution. In our experiments, the flux at the tricrystal point is imaged with a scanning superconducting quantum interference device (SQUID) microscope (SSM). In our SSM, the sample is scanned using a mechanical lever mechanism relative to a well shielded pickup loop integrated into a SQUID sensor [15].

Figures 1(c)–1(e) show SSM images of $N_\phi = \pm 1/2$ vortices at the tricrystal point of a 130 nm thick $Y_{0.7}Ca_{0.3}Ba_2Cu_3O_{7-\delta}$ (Ca-doped Y-123) film epitaxially grown by pulsed laser deposition on a $SrTiO_3$ tricrystal in the geometry of Fig. 1(a). These films have sufficiently high grain boundary supercurrent densities [16] that Josephson vortices in the grain boundaries and at the tricrystal point are resolution limited with a 4 μm diameter pickup loop. The $N_\phi = +1/2$ state can be inverted to the $-1/2$ state [Fig. 1(c)] by applying currents of a few mA with the appropriate polarity through the field coil of the SQUID susceptometer [17].

Integration of the total flux at the tricrystal point [Fig. 1(f)] shows that the $N_\phi = \pm 1/2$ states have the same total flux and field distribution. The TRSB pair states are thus ruled out, provided that the chirality of the order parameter is invariant with the sense of the applied magnetic field; that is that there is no magnetic field induced change in the macroscopic quantum state of the superconductor itself, as opposed to a simple reversal of the circulating supercurrent. The fact that we observed a total flux of $\sim\phi_0/2$ at the tricrystal point can also rule out significant TRSB pair states [18,19].

In contrast to Ca-doped Y-123, La-214 films grown on $SrTiO_3$ tricrystals have relatively low T_c's and very small grain boundary critical current densities, presumably due to the lattice mismatch between the deposited film and the substrate [20]: The fields of the half-fluxon at the tricrystal point for the $T_c = 28.5$ K sample shown in Fig. 2 spread out along the grain boundaries over tens of microns. Nevertheless, it is clear that there are spontaneous currents at the tricrystal point, and that the resulting vortex retains time-reversal symmetry [Fig. 2(b)]. For detailed modeling, the flux/unit length in one branch of the vortex (labeled by i) can be written as [21]

$$\frac{d\phi_i}{dr_i} = \frac{\phi_0}{2\pi}\frac{-4a_i}{\Lambda_{Ji}}\frac{e^{-r_i/\Lambda_{Ji}}}{1 + a_i^2 e^{-2r_i/\Lambda_{Ji}}}, \qquad (2)$$

where r_i is the absolute value of the distance along the ith grain boundary from the tricrystal point, Λ_{J_i} is the Josephson penetration depth of the ith grain boundary, $a_i/[\Lambda_{Ji}(1 + a_i^2)]$ is the same for each grain boundary, and the total flux at the tricrystal point is $\phi = \sum_i(\phi_0/2\pi)4\tan^{-1}(a_i)$. The flux through the SQUID pickup loop is calculated by propagating the fields at the surface to the pickup loop height using Fourier transform techniques, and then integrating over the known pickup loop geometry. Results of fits of these calculations to the data [Fig. 2(c)] show that, to within our experimental errors, the vortex at the tricrystal point has a total flux of $\phi_0/2$. The height of the pickup loop was determined from measurements of bulk vortices. This left

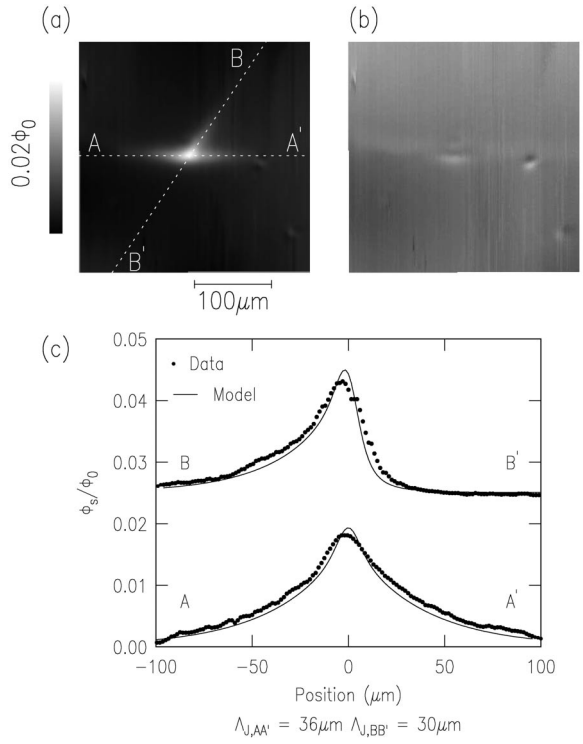

FIG. 2. SQUID microscope images, taken with an 8 μm square pickup loop, of the tricrystal point region for an underdoped ($T_c = 28.5$ K, thickness = 310 nm) La-214 film epitaxially grown by laser ablation. (a) Difference image $[\phi_s(+20\text{ nT}) - \phi_s(-20\text{ nT})]/2$ (to cancel out stray fields) for images taken with the sample cooled in ± 20 nT fields, resulting in $N_\phi = \pm 1/2$ Josephson vortices at the tricrystal point. The sum image $[\phi_s(+20\text{ nT}) + \phi_s(-20\text{ nT})]/2$ (b) shows that the flux from the $N_\phi = \pm 1/2$ vortices cancel out within a few percent. (c) Cross sections through the data of (a), and fits using the Josephson penetration depths Λ_J along the two grain boundaries as fitting parameters, assuming the vortex at the tricrystal point has $\phi_0/2$ of magnetic flux. The best fit value, allowing the total flux at the tricrystal point to vary, was $\phi = (0.585 \pm 0.1)\phi_0$.

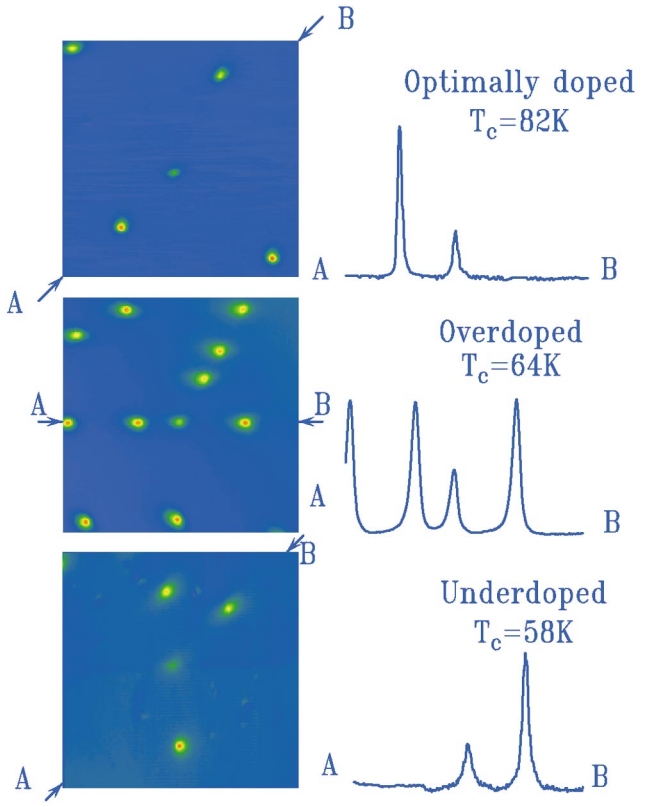

FIG. 3 (color). SQUID microscope images for tricrystal samples with optimally, underdoped, and overdoped $Bi_2Sr_2CaCu_2O_{8+\delta}$ 300 nm thick films epitaxially grown by RF sputtering on a $SrTiO_3$ substrate with the geometry of Fig. 1(a). The images were taken with a 4 μm octagonal pickup loop (optimal) and a 7.5 μm square pickup loop (overdoped and underdoped). Full scale variation in ϕ_s was $0.4\phi_0$, $0.18\phi_0$, and $0.21\phi_0$, respectively. The lines are cross sections of the image data through the tricrystal point along the directions indicated.

three fitting parameters: the two Josephson penetration depths and the total flux in the tricrystal vortex.

Tricrystal experiments were also performed on a number of $Bi_2Sr_2CaCu_2O_{8+\delta}$ (Bi-2212) superconductors with various doping levels achieved by controlling the oxygen content during film deposition, or thermal annealing of a given tricrystal Bi-2212 film [22] (Fig. 3). Modeling like that described above [21] showed that in all cases there was $\phi_0/2$ total flux at the tricrystal point within experimental error, and that the absolute value of the total flux at the tricrystal point remained the same within a few percent when the vortex was inverted, either by applying a local field at low-temperature, or by cooling again in a slightly different field. The crystal structure of all the Bi-2212 samples studied here is tetragonal equivalent [7]. A $d + s$ mixed pair state in Bi-2212 is therefore symmetry forbidden.

It is possible that the dopant concentration at or near the grain boundary is different from the bulk. However, we believe that there is not a significant region with different doping away from the grain boundaries, for several reasons. Numerous studies indicate that the crystal structure in multigrain cuprates is preserved except in a region 1 nm in width along the grain boundaries [23]. In a tricrystal pairing symmetry test on optimally doped YBCO, the grain boundary Josephson penetration depths diverged at the same temperature as the bulk T_c, and the half-flux quantum effect persisted to within 1 K of T_c [24]. Since the coherence length diverges at T_c, this implies that d-wave pairing symmetry extends at least 10 times the low-temperature coherence length into the grains. Further, scanning susceptibility measurements on $Y_{0.7}Ca_{0.3}Ba_2Cu_3O_{7-\delta}$ bicrystals indicate that the supercurrent across the grain boundary has a T_c within 5 K of that in the bulk. In addition, bulk transport measurements are consistent with a model, including phase fluctuations, of transport between two superconductors, with the same T_c as the bulk, separated by a thin insulating region [25].

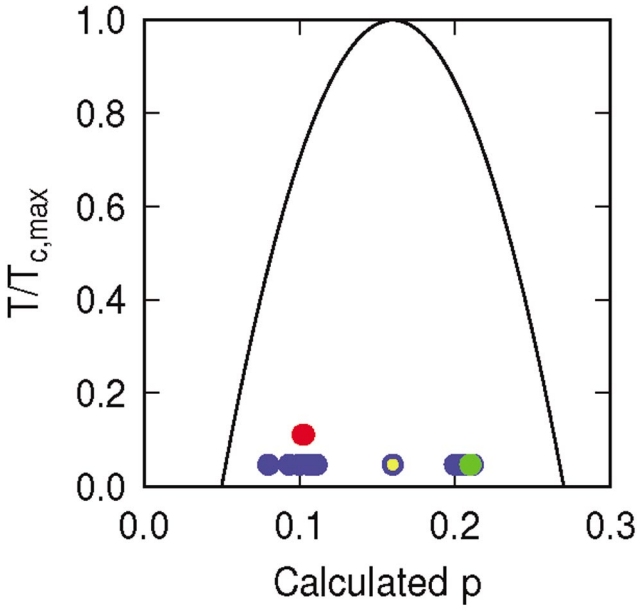

FIG. 4 (color). Plots of $4.2\ \mathrm{K}/T_{c,\max}$ vs p, the calculated doping holes per CuO_2 layer, calculated from the ratio $T_c/T_{c,\max}$ using Eq. (1) (solid line), for the samples reported in this Letter, with $p_c = 0.16$, and $T_{c,\max} = 90$, 90, 38, and 82 K for optimally doped $YBa_2Cu_3O_{7-\delta}$ (yellow dot), $Y_{0.7}Ca_{0.3}Ba_2Cu_3O_{7-\delta}$ (green dot), $La_{1.85}Sr_{0.15}CuO_y$ (red dots), and $Bi_2Sr_2CaCu_2O_{8+\delta}$ (blue dots), respectively.

Finally, a narrow region near the grain boundaries with different symmetry from the bulk (e.g., s vs $d_{x^2-y^2}$) could introduce additional intrinsic π phase shifts at the s-d interfaces, destroying the half-flux quantum effect at the tricrystal point. Therefore it can be argued that the tricrystal experiments are not merely sensitive to the symmetry at our sample interfaces.

Figure 4 displays the doping range covered in this study. Our results show that pairing with $d_{x^2-y^2}$ symmetry is robust in several cuprate systems, over a wide range of doping. Note that $d_{x^2-y^2}$ pairing symmetry in the Bi-2212 system persists to $p \approx 0.07$ (Fig. 4), very close to the onset of superconductivity at $p = 0.05$. At such low doping other orders such as antiferromagnetism, charge density wave and spin density wave phases compete vigorously with d-wave superconductivity [5,6].

As Anderson [26,27] first suggested, the physics of both the normal and superconducting states of the cuprates is dictated by strong Coulomb interactions in the CuO_2 planes. Many theoretical studies including strong correlation effects favor $d_{x^2-y^2}$ over d_{xy} and extended s wave (s^*) states [28,29], with pairing in the $d_{x^2-y^2}$ channel enhanced by on-Cu-site repulsion and suppressed by intersite Coulomb interactions [30].

The robust nature of $d_{x^2-y^2}$ pairing over a wide doping range ($0 < p \leq 0.35$) has been demonstrated by several numerical studies based on Hubbard models [31,32], consistent with our present work. Furthermore, our observation of $d_{x^2-y^2}$ pairing in the low doping regime $p \approx 0.07$ is supported by a recent measurement of c-axis penetration depth as a function of temperature and doping in $YBa_2Cu_3O_{7-\delta}$, suggesting that the $d_{x^2-y^2}$ nodal quasiparticles survive to very low doping [33]. Of interest in the future is the question of the doping dependence of the pairing symmetry in the electron-doped superconductors.

We would like to thank R. Beck, R. H. Koch D.-H. Lee, and D. M. Newns for useful discussions. The work of G. H. and J. M. was supported by the BMBF (13N6918), the DFG (SFB484), and the ESF (PiShift).

[1] J. Orenstein and A. J. Millis, Science **288**, 468 (2000).
[2] M. R. Presland *et al.*, Physica (Amsterdam) **176C**, 95 (1991).
[3] F. F. Balakirev *et al.*, Nature (London) **424**, 912 (2003).
[4] C. Panagopoulos *et al.*, Phys. Rev. B **67**, 220502 (2003).
[5] S. Sachdev, Rev. Mod. Phys. **75**, 913 (2003).
[6] M. Vojta *et al.*, Phys. Rev. B **62**, 6721 (2000).
[7] C. C. Tsuei and J. R. Kirtley, Rev. Mod. Phys. **72**, 969 (2000).
[8] C. Panagopoulos and T. Xiang, Phys. Rev. Lett. **81**, 2336 (1998).
[9] N. -C. Yeh *et al.*, Phys. Rev. Lett. **87**, 87003 (2001).
[10] Y. Dagan and G. Deutscher, Phys. Rev. Lett. **87**, 177004 (2001).
[11] J. A. Skinta *et al.*, Phys. Rev. Lett. **88**, 207005 (2001).
[12] A. Snezhko *et al.*, Phys. Rev. Lett. **92**, 157005 (2004).
[13] P. A. Lee, Phys. Rev. Lett. **71**, 1887 (1993).
[14] J. Takeya *et al.*, Phys. Rev. Lett. **88**, 77001 (2002).
[15] J. R. Kirtley *et al.*, Appl. Phys. Lett. **66**, 1138 (1995).
[16] G. Hammerl *et al.*, Nature (London) **407**, 162 (2000).
[17] B.W. Gardner *et al.*, Rev. Sci. Instrum. **72**, 2361 (2001).
[18] M. Sigrist, Prog. Theor. Phys. **99**, 899 (1998).
[19] M. B. Walker, Phys. Rev. B **62**, 11 854 (2000).
[20] W. Si, H.-C. Li, and X. X. Xi, Appl. Phys. Lett. **74**, 2839 (1999).
[21] J. R. Kirtley *et al.*, Phys. Rev. Lett. **76**, 1336 (1996).
[22] Z. Konstantinovic, Z. Z. Li, and H. Raffy, Physica (Amsterdam) **259B–261B**, 567 (1999).
[23] H. Hilgenkamp and J. Mannhart, Rev. Mod. Phys. **74**, 485 (2002).
[24] J. R. Kirtley, C. C. Tsuei, and K. A. Moler, Science **285**, 1373 (1999).
[25] R. Gross, P. Chaudhari, D. Dimos, A. Gupta, and G. Koren, Phys. Rev. Lett. **64**, 228 (1973).
[26] P.W. Anderson, Science **235**, 1196 (1987).
[27] P.W. Anderson, P. A. Lee, M. Randeria, T. M. Rice, N. Triveda, and F. C. Zhang, cond-mat/0311467, and references therein.
[28] E. Dagotto, Rev. Mod. Phys. **66**, 763 (1994).
[29] N. Bulut, Adv. Phys. **51**, 1587 (2002), and references therein.
[30] E. Plekhanov, S. Sorella, and M. Fabrizio, Phys. Rev. Lett. **90**, 187004 (2003).
[31] A. Paramekanti, M. Randeria, and N. Trivedi, Phys. Rev. Lett. **87**, 217002 (2001).
[32] S. Sorella *et al.*, Phys. Rev. Lett. **88**, 117002 (2002).
[33] H. Hosseini *et al.*, cond-mat/0312542.